UCRL- 84283
PREPRINT

# PLASMA PERFORMANCE STUDY FOR THE TANDEM MIRROR REACTOR

Bruce M. Boghosian

This paper was prepared for inclusion in the Proceedings of the Fourth ANS Topical Meeting on The Technology of Controlled Nuclear Fusion, King of Prussia, PA October 14-17, 1980.

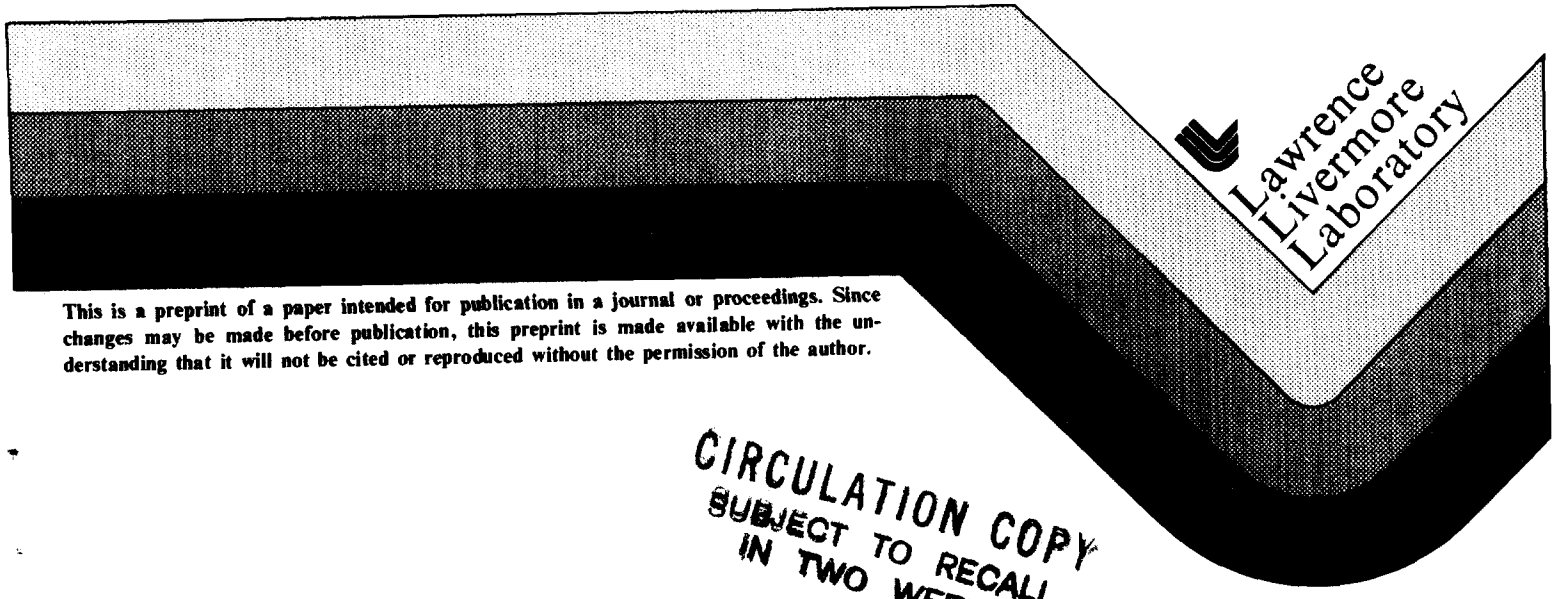

# PLASMA PERFORMANCE STUDY FOR THE TANDEM MIRROR REACTOR*

Bruce M. Boghosian
Lawrence Livermore National Laboratory

## Summary

We have developed a computer code for assessing the performance of new variations on the thermal barrier idea for tandem mirror reactors (TMR's). The code solves the particle and energy balance equations simultaneously for each species of particles in each portion of the machine. The code is thus able to detemine the neutral beam and ECRH injection powers that are required to sustain an equilibrium situation, and, from these, to determine the machine's Q value. This paper focuses on the methodology and numerical algorithms used in accomplishing this solution. We plan to use this code to compare the A-cell barrier TMR with axisymmetric TMR's.

## Introduction

This paper describes a computer code developed at the Lawrence Livermore National Laboratory (LLNL) to assess the performance of two new tandem mirror fusion reactor (TMR) concepts. Both of these new concepts are variations on the thermal barrier idea invented by Baldwin, Logan, and Fowler in April of 1979.[1] As originally proposed, the idea called for a potential depression to be created between the central cell and the plug of a tandem mirror. Such a depression could be obtained by decreasing the magnetic field in this region, and maintained by pumping out the ions that would tend to collisionally trap in the potential depression. This depression reduced the thermal contact between passing central-cell electrons and potential-trapped plug electrons. Because of this reduced thermal contact, it became possible to dramatically increase the plug electron temperature, and hence the plug potential, by modest amounts of electron-cyclotron resonant heating (ECRH) in the plug. This original idea became known as the inside-barrier concept, and a computer code for assessing the performance of tandem mirror reactors with inside thermal barriers was developed in November of 1979.[2]

*Work performed under the auspices of the U.S. Department of Energy by the Lawrence Livermore National Laboratory under contract number W-7405-ENG-48.

Though the inside-barrier concept remains in strong contention and has been actively pursued by the University of Wisconsin, Livermore, for a number of reasons,[3] decided to examine another thermal-barrier configuration, called the A-cell barrier. In addition, Livermore is investigating a novel TMR concept called the axisymmetric cusp, first described by Logan in November, 1979.[4] This paper outlines the physics modeling from LLNL's parametric code for A-cell and axisymmetric-cusp tandem mirror reactors. A detailed description of all the equations in the model and the numerical methods used to solve them is given in Ref. 5.

## Qualitative Description of A-Cell Barriers

The A-cell barrier incorporates a

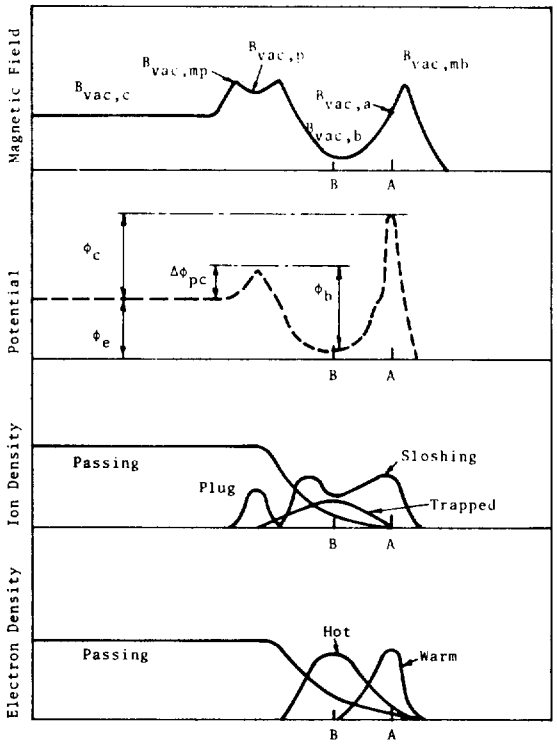


Figure 1 Axial Profiles

neutral-beam-injected yin-yang plug, in which the potential is slightly raised between the central cell and the barrier region. On the outboard side of this plug there is a C-coil. The barrier region lies in the gap between the plug's outboard mirror and the C-coil.

The magnetic field strength, plasma density, and plasma-potential profiles are depicted in Fig. 1. Note that off-minimum injection of ions in the barrier, coupled with ion pumping at the barrier minimum, creates a distribution of sloshing ions with density peaks at either side of the barrier minimum. ECRH heating at the outboard peak (point A) produces the machine's highest potential maximum, which ultimately confines the central-cell ions that pass through the yin-yang plug. This can be seen in the typical velocity-space diagram for central-cell ions, pictured in Fig. 2. The

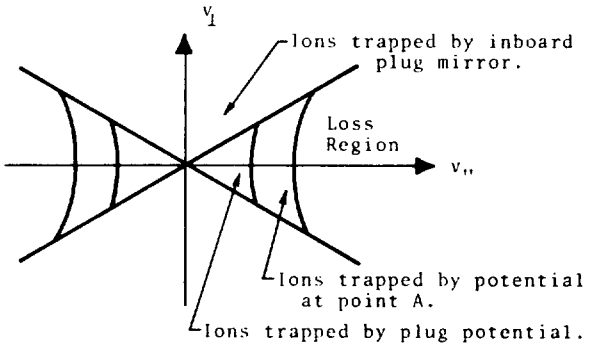


Figure 2 Central Cell Ion Velocity Space

electrons see this point as a potential well, and those electrons that lie within a certain ellipsoidal region of velocity space at point A (Fig. 3) are potentially trapped there, and are referred to as "warm-electrons." Because the ECRH heats electrons in the perpendicular

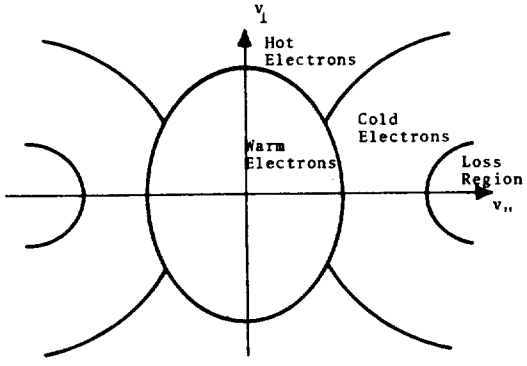


Figure 3 Point A Electron Velocity Space

direction in velocity space, it tends to not only raise the warm-electron temperature, but also to convect them out of the ellipsoidal well. Both of these effects tend to untrap the warm-electrons from the well at point A, and this is why the potential there rises.

Figure 4 shows the velocity-space diagram for electrons at the barrier minimum (point B). ECRH is also applied here because, by convecting electrons in the perpendicular direction in velocity space, it tends to trap them in a mirror well at high energy. These high-energy, mirror-trapped electrons are referred to as hot-electrons, and the effect of maintaining them there is to depress the potential at point B--almost to ground.

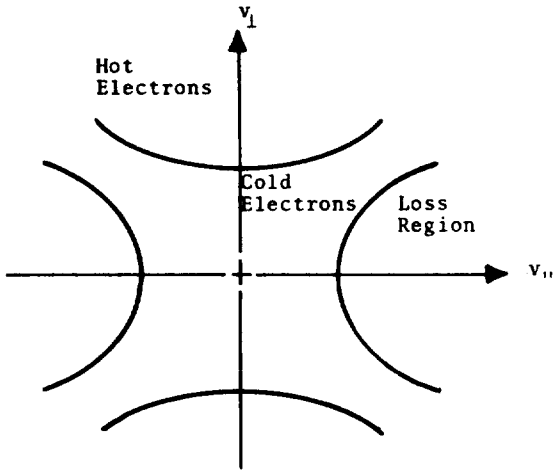


Figure 4 Point B Electron Velocity Space

The axisymmetric TMR, as it was originally proposed,[4] was to work in much the same way as the A-cell barrier TMR; field lines from the central cell were to pass through a plug, in which the potential was slightly raised, into a barrier region. It was later decided not to use a plug in this configuration. In the A-cell barrier configuration, the plug is necessary to provide good curvature for MHD stability; the axisymmetric configuration, however, has good curvature in other places. Thus, in the axisymmetric-TMR physics model the central cell is adjacent to the barrier region.

## Outline of A-Cell Barrier Physics

The code's treatment of the central-cell physics is nearly identical to that of the inside-barrier code,[2] with one important addition: the code divides the central cell into concentric flux tubes of equal thickness, and uses magnetic flux conservation to map these flux tubes into the plug and barrier regions. Although the code is not truly one-dimensional in that it does not treat radial diffusion

processes, it does allow the specification of radial beta profiles in the central cell, plug, and barrier (point B) regions. Given these, it solves all subsequent equations, including the particle and energy balance equations, separately along each flux tube.

The Logan-Rensink plug model,[6] coupled with the plug beta equation and plug ion energy balance, is used to determine a self-consistent solution for the plug potential rise $\Delta\phi_{pc}$, the plug density $n_p$, and the plug ion confinement $(n\tau)_p$ along each consecutive flux tube.

To proceed, the central-cell potential $\phi_e$ and the barrier (point A) potential rise $\phi_c$ are guessed. Later, we shall use the central-cell electron and ion particle balances, respectively, to adjust these guesses; this computational structure will be referred to as the "outer loop."

Given $\phi_e$ and $\phi_c$, we then guess the fraction $F_{ec}$ of electrons at point B that are cold (passing). Later, we shall use the hot-electron particle balance to adjust this guess; this computational structure will be referred to as the "middle loop."

Next we guess the barrier potential depression $\phi_b$. We shall now use the quasineutrality condition at point B to adjust this guess; this computational structure will be referred to as the "first inner loop." Given $\phi_b$, the passing-ion density at B is modeled by the following (approximate) mapping equation:

$$n_{ib,pass} = n_{ip,pass}\,\frac{1}{R_{ib}}\left(\frac{T_c}{\pi\phi_b + T_c}\right)^{1/2}, \qquad (1)$$

where $n_{ip,pass}$ is the passing-ion density in the plug (obtained from the plug model), $R_{ib}$ is an effective barrier mirror ratio depending upon the plug and barrier vacuum fields as well as $\Delta\phi_{pc}$ and $T_c$, and $T_c$ is the central-cell ion temperature.

Next, the following two quantities are input (possibly functions of radius):

$$g_{ib} \equiv \frac{n_{ib,pass} + n_{ib,trap}}{n_{ib,pass}} \qquad (2a)$$

and

$$G_{ib} \equiv \frac{n_{ib,pass} + n_{ib,trap} + n_{ib,slosh}}{n_{ib,pass}}, \qquad (2b)$$

so that

$$1 < g_{ib} < G_{ib}, \qquad (2c)$$

and where $n_{ib,trap}$ is the density of ions that are potential-trapped at barrier point B, and $n_{ib,slosh}$ is the density of sloshing ions at barrier point B. Thus, since we know $n_{ib,pass}$:

$$n_{ib,trap} = (g_{ib} - 1)\, n_{ib,pass} \qquad (3a)$$

and

$$n_{ib,slosh} = (G_{ib} - g_{ib})\, n_{ib,pass}, \qquad (3b)$$

so the total ion density at point B is

$$n_{ib} = G_{ib}\, n_{ib,pass} \quad . \qquad (3c)$$

Now, the cold (passing) electron density at point B is given by the mapping equation:

$$n_{eb,cold} = n_{ep}\left[\frac{\exp\left(-\frac{\phi_b}{T_{ec}}\right) - \exp\left(-\frac{\phi_e + \Delta\phi_{pc}}{T_{ec}}\right)}{1 - \exp\left(-\frac{\phi_e + \Delta\phi_{pc}}{T_{ec}}\right)}\right], \qquad (4)$$

where $n_{ep}$ is the plug electron density (obtained from the plug model), and $T_{ec}$ is the central-cell electron temperature. The hot-electron density at barrier point B is then given by:

$$n_{eb,hot} = n_{eb,cold}\left(\frac{1 - F_{ec}}{F_{ec}}\right), \qquad (5a)$$

so the total electron density at point B is:

$$n_{eb} = n_{eb,cold}/F_{ec} \quad ; \qquad (5b)$$

these two equations follow directly from the definition of $F_{ec}$. Combining Eq. (1), (3c), (4), and (5b), the quasineutrality condition, $n_{ib} = n_{eb}$, may be written:

$$\phi_b = -T_{ec}\,\ln\left\{\frac{F_{ec}G_{ib}}{R_{ib}}\left(\frac{n_{ip,pass}}{n_{ep}}\right)\left(\frac{T_c}{\pi\phi_b + T_c}\right)^{1/2}\left[1 - \exp\left(-\frac{\phi_e + \Delta\phi_{pc}}{T_{ec}}\right)\right] + \exp\left(-\frac{\phi_e + \Delta\phi_{pc}}{T_{ec}}\right)\right\} \qquad (6)$$

This can be solved by a fixed-point iteration: that is, Eq. (6) may be used to obtain a better estimate of $\phi_b$, and the first inner loop is repeated with this new estimate until convergence is obtained. Once we have $\phi_b$, the potential drop from point A to point B, $\delta\phi_a$, is given by:

$$\delta\phi_a = \phi_b + \phi_c - \Delta\phi_{pc} \quad . \qquad (7)$$

Next, we guess the value of beta at point A, $\beta_a$. We shall now use the warm electron particle balance to adjust this guess; this computational structure will be referred to as the "second inner loop." Given $\beta_a$, the beta-reduced magnetic field at point A is:

$$B_{pla,a} = B_{vac,a}\left(1-\beta_a\right)^{1/2} \quad . \tag{8}$$

We may now write the beta equation at point A:

$$\left(n_{ib,pass} + n_{ib,trap}\right)\frac{T_c}{R_{ib}} + n_{ec,b}\,T_{ec} + n_{ib,slosh}\,E_{inj,a}\,\frac{B_{pla,b}}{B_{pla,a}} + n_{eb,hot}\,0.8\,\bar{E}_{eh} = \left(\frac{B^2_{vac,b}}{2\mu_0}\right)\beta_b \quad . \tag{9}$$

The first term on the left is the pressure contribution from both passing and trapped ions (this is reduced by the factor $R_{ib}$ since we are interested only in the perpendicular pressure). The second term is the cold-electron pressure, the third term is the sloshing-ion perpendicular pressure, and the fourth term is the hot-electron perpendicular pressure. In the fourth term, $\bar{E}_{eh}$ is the mean hot-electron energy, and the factor of 0.8 is used instead of 2/3 because, being mirror-trapped, most of the hot-electron pressure is perpendicular. We can solve Eq. (9) for $\bar{E}_{eh}$, since we know everything else.

Next, the cold electrons, hot electrons, and sloshing ions are mapped from point B to point A by the following (approximate) relations:

$$n_{ea,cold} = n_{eb,cold}\left(\frac{B_{pla,a}}{B_{pla,b}}\right)\left(\frac{T_{ec}}{\pi\delta\Phi_a + T_{ec}}\right)^{1/2}, \tag{10}$$

$$n_{ea,hot} = n_{eb,hot}\left(\frac{B_{vac,mb} - B_{pla,a}}{B_{vac,mb} - B_{pla,b}}\right)\left(\frac{0.2\,\bar{E}_{eh}}{0.2\,\bar{E}_{eh} + \delta\Phi_a}\right)^{1/2}, \tag{11}$$

and

$$n_{ia,slosh} = n_{ib,slosh}\left(\frac{B_{pla,a}}{B_{pla,b}}\right)^{x}\left(\frac{E_{inj,a} + \delta\Phi_a}{E_{inj,a}}\right)^{1/2}, \tag{12}$$

respectively. In Eq. (11), $B_{vac,mb}$ is the vacuum field at the barrier mirror (see Fig. 1). Also, the factor 0.2 in front of $\bar{E}_{eh}$ is meant to give the parallel-energy component. In Eq. (12), x is an exponent chosen to model the charge-exchange pumping effect on the sloshing-ions; in our studies thus far we have used x = 1.

The quasineutrality condition at point A can then be invoked to find the warm-electron density:

$$n_{ea,warm} = n_{ia,slosh} - n_{ea,cold} - n_{ea,hot}. \tag{13}$$

Note that the passing and trapped-ion densities go to zero at point A.

Next, we employ the beta equation at point A:

$$n_{ia,slosh}\,E_{inj,a} + n_{ea,warm}\,T_{ew} + n_{ea,cold}\,T_{ec} + n_{ea,hot}\,0.8\,\bar{E}_{eh} = \left(\frac{B^2_{vac,a}}{2\mu_0}\right)\beta_a \quad , \tag{14}$$

where $E_{inj,a}$ is the sloshing-ion injection energy. This equation may be solved for $T_{ew}$ since everything else is known.

We now know everything we need to know to check the warm-electron particle balance. Warm-electrons are introduced by the sloshing-ion beam, the current of which is calculated from the sloshing-ion particle balance and the low-energy pump beam. Warm-electrons are also introduced when cold (passing) electrons trap in the ellipsoidal well. The collisional loss of electrons from an ellipsoidal well in velocity space has been modeled by Cohen, et al.[7] Under conditions of strong ECRH, all exiting electrons emerge as hot-electrons with perpendicular energy $\delta\Phi_a/(1 - R_{ab})$, where $R_{ab}$ is $B_{pla,b}/B_{pla,a}$; under conditions of weak ECRH, some exiting electrons emerge as cold (passing) electrons as well (see Fig. 3).

The mathematical details of this model will be found in Ref. 5. For now we note that when all these entering and exiting currents are calculated, they will not, in general, balance. Thus, we must adjust our guess for $\beta_a$ until they do. This completes the second inner loop.

Next, we check the hot-electron particle balance. Hot-electrons are produced when ECRH at point A boils electrons out of the top of the ellipsoidal well there (recall this was a loss term for the warm-electrons). Hot-electrons can also be produced by the ECRH applied at point B, because it convects cold (passing) electrons upwards in perpendicular energy until they mirror-trap (see Fig. 4). These two source currents are balanced against the confinement loss of electrons in a mirror well. The value that was guessed for $F_{ec}$ is adjusted until the terms do, indeed, balance. This completes the middle loop.

We may think of the middle and inner loops as an attempt to solve two equations, the warm- and hot-electron particle balance equations, in two unknowns, $F_{ec}$ and $\beta_a$. It turns out that this solution is not easy. Fixed-point iterations definitely do not work here. The existence of multiple solutions, which have been found under certain circumstances, foils bisection or regula falsi techniques (neither of which are well suited to two-dimensional root finding anyway). Newton step techniques can run into trouble because in the domain, $0 < F_{ec} < 1$ and $0 < \beta_a < 1$, there may be points for which the balance equations' terms are undefined. For example, if $\beta_a$ gets too big, Eq. (9) can yield a negative value for $\bar{E}_{eh}$; if $\beta_a$ gets too small, on the other hand, Eq. (14) can yield a negative value for $T_{ew}$. At present, the code scans the entire domain looking for a solution at each point, and, if there are multiple solutions, selects the solution with the smallest $\beta_a$ at the smallest $F_{ec}$. This

process is time-consuming, but it seems to work. Work to find a speedy, reliable algorithm to solve these equations is ongoing.

The central-cell ion and electron particle and energy balance equations are next solved for the central-cell auxiliary ion-fueling current, the auxiliary cold-electron current (described in Ref. 1), and the fractions of trapped ions pumped by the low-, medium-, and high-energy pump beams. Only two of the pump-beam fractions are independent (the third is determined by the condition that all three should add to one), so this gives us four equations in four unknowns. These are linear equations (for this choice of unknowns) and so they can be easily solved. We then adjust our initial guesses for $\phi_e$ and $\phi_c$ until the pump-beam fractions come out to be what we want them to be. This adjustment is done by means of Powell's technique for finding roots (a compromise between a Newton step and a steepest descent step), and the Jacobian is updated at each step according to Broyden's method.[8] This completes the outer loop.

The neutral beam current input to the plug is calculated from the plug ion-particle balance, and from this we can find the plug injection power. The neutral-beam current input to the barrier (sloshing-ion beam) is found from the sloshing-ion particle balance, and the sloshing-ion beam injection power is calculated. A trapped-ion particle balance, in conjunction with the three pump-beam fractions, fixes the currents of each of the three beams, and thus determines the injected pumping power. The ECRH power inputs at A and B are calculated from the warm- and hot-electron energy balances, respectively.

It should be borne in mind that all of the above is done for each flux tube separately, and the results are integrated over the radial profile to get the total input power. This total input power is then divided into the fusion power to get the plasma Q. We also note that the code, as it is currently structured, tells us what current and ECRH radial-deposition profiles are necessary to achieve the input beta profiles.

## Status of Code

We plan to use the code to quantify a comparison study between the axisymmetric and A-cell barrier configurations of tandem mirror reactors. Though the former may achieve higher central-cell beta values, it may necessitate higher pumping power than the A-cell design because the latter's potential rise, $\Delta\phi_{pc}$, serves to attenuate the number of passing ions that enter the barrier region.

Numerical results in the form of test cases and/or parametric studies are not yet available. The code's inner and middle loops have converged successfully, but not in conjunction with a fully physically-consistent solution to its outer loop. It is not yet clear whether this failure to converge is due to algorithmic difficulties, to problems with the physics model, or to inconsistencies in the input data used thus far.

## References


1. D. E. Baldwin, B. G. Logan, and T. K. Fowler, An Improved Tandem Mirror Fusion Reactor, Lawrence Livermore National Laboratory, Livermore, CA, UCID-18156 (1979).

2. B. M. Boghosian, D. A. Lappa and B. G. Logan, Physics Parameter Calculations for a Tandem Mirror Reactor with Thermal Barriers, Lawrence Livermore National Laboratory, Livermore, CA, UCID-18314 (1979).

3. G. A. Carlson, "The Design of Tandem Mirror Reactors with Thermal Barriers," these Proceedings.

4. B. G. Logan, An Axisymmetric, High Beta Tandem Mirror Reactor, Lawrence Livermore National Laboratory, Livermore, CA, UCRL-83555 (1979).

5. UCID in preparation.

6. G. A. Carlson, et al, Tandem Mirror Reactor with Thermal Barriers, Lawrence Livermore National Laboratory, Livermore, CA, UCRL-52836 (1979), pp. 48-51.

7. R. H. Cohen, et al, Particle and Energy Exchange Between Untrapped and Electrostatically Confined Populations in Magnetic Mirrors, Lawrence Livermore National Laboratory, Livermore, CA, UCRL-84147 (1980).

8. M.J.D. Powell, A Fortran Subroutine for Solving Systems of Non-Linear Algebraic Equations, AERE-R-5947 (1968).